JOURNAL OF THEORETICAL AND APPLIED MECHANICS
51, 3, pp. 763-774, Warsaw 2013

INFLUENCE OF IDEAL AND NON-IDEAL EXCITATION SOURCES ON THE DYNAMICS OF A NONLINEAR VIBRO-IMPACT SYSTEM

Fernando H. Moraes, Bento R. Pontes Jr, Marcos Silveira
UNESP – São Paulo State University, Department of Mechanical Engineering, Bauru, SP, Brazil
e-mail: brpontes@feb.unesp.br

José M. Balthazar
UNESP – São Paulo State University, Department of Mechanical Engineering, Bauru, SP, Brazil and
UNESP – São Paulo State University, IGCE, Department of Applied Mathematics and Computation, Rio Claro, SP, Brazil

Reyolando M.L.R.F. Brasil
Federal University of ABC, Santo André, SP, Brazil

The objective of the present work is to analyze the dynamics of a vibro-impact system consisting of two blocks of different mass coupled by a spring with two stages. Two different types of excitation sources for the system are used in the analysis: the first is an ideal excitation in form of a harmonic force, and the second is a non-ideal excitation in form of a DC electric motor with limited power supply which has an unbalanced rotor. The control parameter for both situations is the excitation frequency of the system. The analysis includes time histories of displacements and velocities, phase portraits and diagrams of the displacement and frequency, used to show the Sommerfeld effect. For certain values of the parameters of the system, the motion is chaotic. The mathematical model of the system is used to obtain an insight to the global dynamics of the vibro-impact system. The model with a non-ideal excitation is more realistic, complete and complex than the model with the ideal excitation.

Key words: vibro-impact system, limited power supply, non-ideal excitation, Sommerfeld effect

1. Introduction

There are many applications in engineering where it is necessary the use impacts to induce vibrations in parts of the system in order to improve its performance or efficiency. The vibro--impact mechanisms deserve as much attention as well as vibration absorbers, since they are present in a wide range of systems in mechanical, civil, and electrical engineering. Examples of applications are vibratory conveyors, drilling machines, compacting machines, forging hammers, impact hammers and powder mixers. Souza *et al.* (2008) considered vibro-impact systems which have many implementations in applied mechanics, ranging from drilling machinery and metal cutting processes to gearboxes. Moreover, from the point of view of dynamical systems, vibro--impact systems exhibit a rich variety of phenomena, including chaotic motion.

Pavlovskaia *et al.* (2001) conducted studies in a vibro-impact system of two degrees of freedom and stated that although it seems simple, the dynamics of the system is very complex, ranging from periodic regimes to chaotic regimes. Ing *et al.* (2010) performed extensive experimental investigations of an impact oscillator with a one-sided elastic constraint. Different bifurcation scenarios have been shown for a number of values of the excitation amplitude, with the excitation frequency as the bifurcation parameter.

Lin and Ewins (1993) performed detailed numerical and experimental studies on chaotic vibration of mechanical systems with backlash. The backlash, in such systems, arise in engineering systems in which components make intermittent contact due to the existence of clearances

(or gaps). The forcing parameter range for the existence of chaotic regime and the influence of damping on the chaotic behavior were investigated.

A major application of vibro-impact mechanisms can be seen in soil drilling machines, or oil drilling, due to high costs involved in these types of projects, with a drill that may have more than kilometers of length and has multiple vibration modes (Wiercigroch *et al.*, 2005). In this case, any kind of failure or maintenance is highly complex and expensive.

Very often the drilling operation does not allow error. Aguiar (2010) conducted studies focused on oil drilling, where a condition of impact on the interaction between the drill and the rock is able to facilitate the penetration by spreading cracks in the hard rock to be drilled. The drilling of brittle materials requires a high rate of energy transfer to induce fracture of the material to be drilled. The most suitable transfer of energy between the drill bit and the rock is by impact.

The energy sources can be classified as ideal and non-ideal. The ideal energy sources do not consider that the acting forces on the system influence the motor dynamics, the models that use the ideal excitation are simplified models that disregard important phenomena. Thus, a model that uses a non-ideal energy source is a significantly more complete and complex model.

Kononenko (1969) described the first type of the non-ideal problem, the Sommerfeld effect, first seen in 1904. The Sommerfeld effect is due to the excitation source having limited power, usually called a non-ideal source. Nayfeh and Mook (1979) obtained analytical solutions for various non-ideal problems, which are composed of oscillators connected to this form of energy source. Dimentberg *et al.* (1997) analised the dynamics of an unbalanced shaft interacting with a limited power supply. Numerical and experimental solutions were obtained, and extensive parametric studies were performed on the Sommerfeld effect.

The main influence of the non-ideal energy source on the system is notable as it passes through resonance. As the power supplied to the source increases in the region before resonance, the angular velocity of the energy source increases accordingly. Near the resonance, it appears that additional power supplied to the motor will only increase the amplitude of the oscillating system response, with little effect on the angular velocity of the energy source. As a consequence, the non-ideal oscillating system cannot pass through the resonance frequency of the system, or requires an intensive interaction between the vibrating system and the energy source to be able to do so (Balthazar *et al.*, 2003; Zukovic and Cvetićanin, 2007, 2009).

Souza *et al.* (2005a,b) investigated numerically the dynamical behavior of a non-ideal mechanical system comprised of an oscillating mass body excited by an unbalanced rotor driven by a non-ideal motor, containing another mass which can oscillate back and forth, colliding with the walls of the main mass. The motor and the unbalanced rotor represent a limited energy source. The dynamics of the oscillating system is largely influenced by the limited energy source.

Warminski *et al.* (2001) investigated vibrations of parametrically and self-excited systems with ideal and non-ideal energy sources. Tsuchida *et al.* (2005) studied dynamics of a non-ideal system with two coupled oscillators. The analysis of the responses showed that for certain values of the parameters in the resonant regime, jump phenomena occur and chaos appears. Zukovic and Cvetićanin (2007, 2009) analysed dynamics of a non-ideal system comprised of an oscillator connected with an unbalanced motor with clearance. The transient and steady state responses and stability were studied. The Summerfeld effect was detected, and chaotic regimes were found for a range of parameters.

The occurrence of chaos in non-ideal systems is associated with the presence of non-linear terms, bifurcation points, instability regions and non-stationary regimes in the resonance region as well as abrupt transitions in stiffness. Therefore, it is of great importance to study the system in those regions.

A DC electric motor with limited power supply is considered as a non-ideal source of energy (Balthazar *et al.*, 2005). The influence of the response of the flexible structure on the DC motor

causes the appearance of a jump phenomenon and the Sommerfeld effect. The DC motor has a family of static characteristic curves, each being associated with a torque constant and with an angular velocity constant of the motor. The manner of regulation, more usual, is the variation of voltage applied to the motor terminals, which controls the angular velocity. The angular velocity affects the motor torque.

This paper is organised as follows. Section 2 contains the mathematical models of the two vibro-impact systems used in this work, the first uses an ideal excitation source, the second uses a non-ideal excitation source. Section 3 contains the results from numerical simulations of both models, including time histories of displacements and velocities, phase portraits and diagrams of the displacement and frequency, used to show the Sommerfeld effect for the model with the non-ideal excitation.

2. Mathematical modeling

Two cases are presented and analysed. The first (Case I) involves a vibro-impact model with the ideal excitation. The excitation source is a harmonic force (F_h) acting on block 1, and the control parameter is the excitation frequency (ω) related to this force. The second (Case II) involves a vibro-impact model with a non-ideal excitation. The excitation comes from a DC electric motor with limited power supply and an unbalanced rotor, and the control parameter is the angular velocity constant of the motor (Ω_0). This model differs from the previous one only by the type of excitation source.

2.1. Model with ideal excitation

The model with ideal excitation has two degrees of freedom and consists of two blocks (1 and 2) with mass m_1 and m_2, respectively, with m_2 greater than m_1. They are coupled by a spring with elastic stiffness coefficient k_1 and a viscous damper with damping coefficient c. The displacements of blocks 1 and 2 are given by x_1 and x_2, respectively. The model is shown in Fig. 1

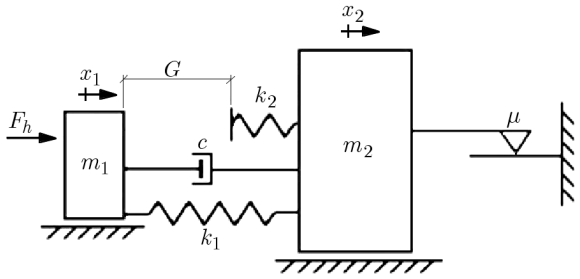

Fig. 1. Vibro-impact model with ideal excitation

A harmonic force F_h provides a sinusoidal excitation on block 1. Block2 has an extension subject to the dry friction force against a surface, with dry friction coefficient μ. This friction generates a counter force to the displacement. In application to drilling machines, the dry friction represents the interaction between the drill and the surface.

A secondary spring (impact spring) exists between the two blocks, with a very high stiffness compared to the first spring. The elastic constant k_2 of the second spring represents the stiffness of the material of block 2.

Springs 1 and 2 form together a spring system with two stages of stiffness. As the elastic constant k_2 is much greater than the elastic constant k_1, there is an abrupt transition in the stiffness as block 1 makes or loses contact with the second spring (Fig. 2). The gap G is the distance between block 1 and the point of contact with the second spring. Whenever the

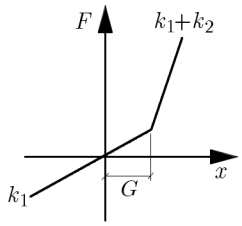

Fig. 2. Two-stage stiffness characteristic of the spring system (Zukovic and Cvetićanin, 2009)

relative displacement between the blocks is smaller than this gap, impact occurs. The system behaves periodically when there is no abrupt stiffness transition in the two-stage spring, when the relative displacement between the blocks is smaller than the gap G. Figure 2 shows the stiffness characteristic of the two-stage spring system (Zukovic and Cvetićanin, 2009):
— while there is no impact on the system, meaning $x_2 - x_1 < G$, the equations of motion are

$$m_1\ddot{x}_1 = F_h - F_{s1} - F_d \qquad m_2\ddot{x}_2 = F_{s1} + F_d - F_f \tag{2.1}$$

— when the relative displacement between the blocks is greater than the gap, meaning $x_2 - x_1 \geqslant G$, impact occurs, and the equations of motion are

$$m_1\ddot{x}_1 = F_h - F_{s1} - F_{s2} - F_d \qquad m_2\ddot{x}_2 = F_{s1} + F_{s2} + F_d - F_f \tag{2.2}$$

From these equations, it is possible to see that the system is piecewise linear, consisting of two regions defined by the relationship between the relative displacement $x_2 - x_1$ and the gap G.

The harmonic force (F_h) acting on block 1 has the form

$$F_h = A\sin(\omega t) \tag{2.3}$$

in which A is the amplitude and ω is the frequency of excitation.

The force of the first spring (F_{s1}) is given by

$$F_{s1} = k_1(x_1 - x_2) \tag{2.4}$$

in which k_1 is the elastic constant of this spring, x_1 and x_2 are the displacements of blocks 1 and 2, respectively.

The force of the second, or impact, spring (F_{s2}) is given by

$$F_{s2} = k_2(x_1 - x_2 + G) \tag{2.5}$$

in which k_2 is the elastic constant of this spring and G is the distance between block 1 and the point of contact with this spring.

The viscous damping force (F_d) is given by

$$F_d = c(\dot{x}_1 - \dot{x}_2) \tag{2.6}$$

in which c is the viscous damping coefficient, $\dot{x}_1$ and $\dot{x}_2$ are the velocities of blocks 1 and 2, respectively.

The dry friction force is given by

$$F_f = \mu m_2 g\,\mathrm{sgn}\,(\dot{x}_2) \tag{2.7}$$

in which μ is the dry friction coefficient, g is the acceleration of gravity and $\mathrm{sgn}\,(\cdot)$ denotes the signum function.

This mathematical model has a kinematic compatibility condition: it is not valid when the absolute position of block 1 is greater than the absolute position of block 2. This condition ensures that the blocks do not reverse position. Also, there is no possibility of a block going through the other. Otherwise, the model would be physically inconsistent.

Dimensional parameters $(m_1,\ m_2,\ k_1,\ k_2,\ c,\ \mu,\ G,\ A,\ \omega)$ were based on the model from Ho *et al.* (2010). Three simulations were performed for this case, with $\omega = 3.5\,\text{Hz}$, $\omega = 5.5\,\text{Hz}$ and $\omega = 6.5\,\text{Hz}$. Values of the control parameter (ω) were obtained in a manner that the system shows periodic, quasi-periodic and chaotic responses, with and without the occurrence of abrupt transition of stiffness.

2.2. Model with non-ideal excitation

The model with non-ideal excitation has three degrees of freedom, with the third degree of freedom being the angular position ϕ of the unbalanced rotor of the DC motor. All other aspects of this model are the same as the model with ideal excitation. Figure 3 shows the vibro-impact model with non-ideal excitation.

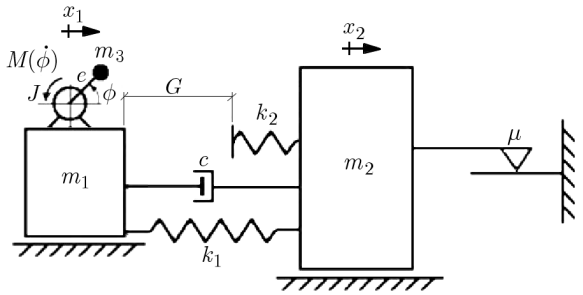

Fig. 3. Vibro-impact model with non-ideal excitation

Block 1 is now excited by a motor which has an unbalanced rotor, with unbalanced mass m_3, eccentricity e and moment of inertia J. This motor is characterized as a non-ideal source. The dimensional parameters $(m_1,\ m_2,\ k_1,\ k_2,\ c,\ \mu,\ G)$ of the model with the non-excitation source are equal to the model with the ideal excitation source.

The torque provided by the motor, $M(\dot{\phi})$, is a function of the angular velocity of the rotor axis with an unbalanced rotor, and is given by

$$M(\dot{\phi}) = M_0\Big(1 - \frac{\dot{\phi}}{\Omega_0}\Big) \tag{2.8}$$

in which M_0 is the torque constant of the motor, $\dot{\phi}$ is the angular velocity of the rotor and Ω_0 is the angular velocity constant of the motor.

The equations of motion valid while there is no impact $(x_2 - x_1 < G)$ are

$$\begin{aligned}
&(m_1 + m_3)\ddot{x_1} = m_3 e(\ddot{\phi}\sin\phi + \dot{\phi}^2\cos\phi) - F_{s1} - F_d\\
&m_2\ddot{x}_2 = F_{s1} + F_d - F_f\\
&(J + m_3 e^2)\ddot{\phi} = m_3 e\ddot{x}_1\sin\phi + M(\dot{\phi})
\end{aligned} \tag{2.9}$$

in which m_3 is the unbalanced mass of the rotor, e is the eccentricity, ϕ is the angular position of the unbalanced mass, J is the moment of inertia of the motor and $M(\dot{\phi})$ is the torque provided by the motor.

When the relative displacement between the blocks is greater than the gap $(x_2 - x_1 \geqslant G)$ impact occurs, and the equations of motion are

$$\begin{aligned}
&(m_1 + m_3)\ddot{x}_1 = m_3 e(\ddot{\phi}\sin\phi + \dot{\phi}^2\cos\phi) - F_{s1} - F_{s2} - F_d \\
&m_2\ddot{x}_2 = F_{s1} + F_{s2} + F_d - F_f \\
&(J + m_3 e^2)\ddot{\phi} = m_3 e\ddot{x}_1 \sin\phi + M(\dot{\phi})
\end{aligned} \tag{2.10}$$

The forces F_{s1}, F_{s2}, F_d, F_f and the torque $M(\dot{\phi})$ are defined in Eqs. (2.4), (2.5), (2.6), (2.7) and (2.8), respectively.

The dimensional parameters of the non-ideal excitation source (m_3, e, J, M_0 and Ω_0) were obtained such that the force of the non-ideal excitation is similar to the force of the ideal excitation, for a better comparison between the models.

The angular velocity constant of the motor (Ω_0) was adopted as the control parameter because it is one of the easiest variables to change in a real experiment with a non-ideal excitation source (DC electric motor). Its variation is achieved by altering the current or voltage on the electric motor.

Three values of the angular velocity constant are used for this case: $\Omega_0 = 3.5\,\text{Hz}$, $\Omega_0 = 5.5\,\text{Hz}$ and $\Omega_0 = 6.5\,\text{Hz}$. The control parameter values were obtained in a way that the first value (3.5 Hz) is below the natural frequency, the second (5.5 Hz) and the third (6.5 Hz) are above the value of the natural frequency of the vibro-impact model $(\omega_n = 4.1\,\text{Hz})$.

It is possible to analyze the influence of the angular velocity constant of the motor relative to capture and passage through the resonance frequency. To this end, three curves were determined representing the DC electric motor based on the angular velocity achieved at the steady state of the motor. Each characteristic curve shows that the motor reaches equilibrium for the system operating at different angular velocities (Fig. 4). The torque constant was kept fixed and the angular velocity constant of the motor (Ω_0) was varied.

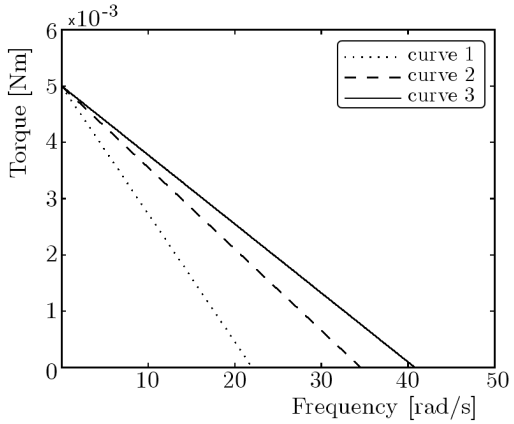

Fig. 4. Motor characteristic curves used in Case II

The analysis includes time histories of displacements and velocities, phase portraits and diagrams of displacement and frequency, used to show the Sommerfeld effect.

A relationship between the harmonic force of the model with ideal excitation and the force provided by the unbalanced rotor has to be established to make a realistic comparison between the models. Recalling Eq. (2.3) and relating it to the force generated by the unbalanced rotor $(m_3 e\omega^2 \sin(\omega t))$, this relationship is expressed by

$$A\sin(\omega t) = m_3 e\omega^2 \sin(\omega t) \qquad A = m_3 e\omega^2 \tag{2.11}$$

The left side of Eq. $(2.11)_1$ corresponds to the ideal excitation force, and the right side corresponds to the non-ideal excitation force. Thus, for each value of the unbalanced mass, the

rotor generates a specific excitation force. Each characteristic curve of the motor determines an angular velocity of the motor axis where the motor reaches the steady state.

The parameters common to the model with the ideal excitation and the model with the nonideal excitation were used with the following values: $m_1 = 0.297\,\text{kg}$, $m_2 = 2.94\,\text{kg}$, $k_1 = 200\,\text{N/m}$, $k_2 = 12400\,\text{N/m}$, $c = 0.001\,\text{Ns/m}$, $\mu = 0.001$ and $G = 0.001\,\text{m}$. The parameters exclusive to the model with the non-ideal excitation were used with the following values: $m_3 = 0.03\,\text{kg}$, $e = 0.11\,\text{m}$, $J = 0.001\,\text{kgm}^2$ and $M_0 = 0.005\,\text{Nm}$.

Table 1 shows the dimensional parameters for the numerical simulations performed in Cases I and II. The symbol '–' used in the table indicates that the value does not exist.

Table 1. Parameter values of the excitation sources used in Cases I and II

Symbol	Case I			Case II		
	A	B	C	A	B	C
A [m]	0.0725	0.1140	0.1350	–	–	–
ω [Hz]	3.5	5.5	6.5	–	–	–
Ω_0 [Hz]	–	–	–	3.5	5.5	6.5

3. Numerical results

The displacements x_1 and x_2 of the system with the ideal excitation source are shown in Figs. 5a, 6a and 7a, with the frequency of 3.5 Hz, 5.5 Hz and 6.5 Hz, respectively. The overall displacement rate of the system increases reasonably as the frequency is increased. Detailed views of these displacements are shown in Figures 5b, 6b, 7b. In these figures, it is possible to see the points where the impact occurs. As the frequency is increased and reaches 6.5 Hz, the impacts are more frequent and start occurring at every cycle. This can be the cause of the perceived increase in the displacement rate.

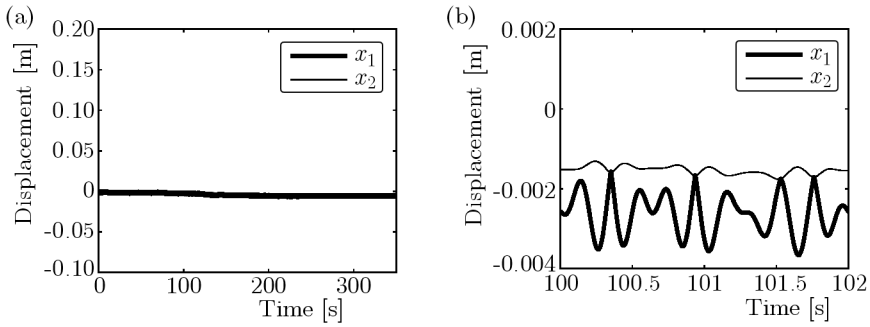

Fig. 5. Displacements of blocks 1 and 2 of the system with ideal excitation with the frequency of 3.5 Hz (a) and a detailed view showing impacts (b)

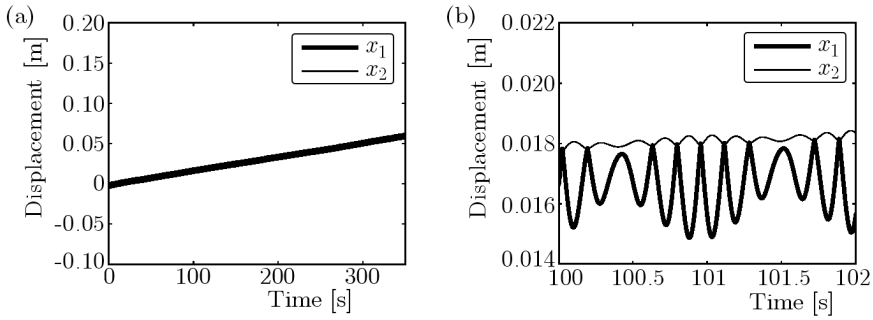

Fig. 6. Displacements of blocks 1 and 2 of the system with ideal excitation with the frequency of 5.5 Hz (a) and a detailed view showing impacts (b)

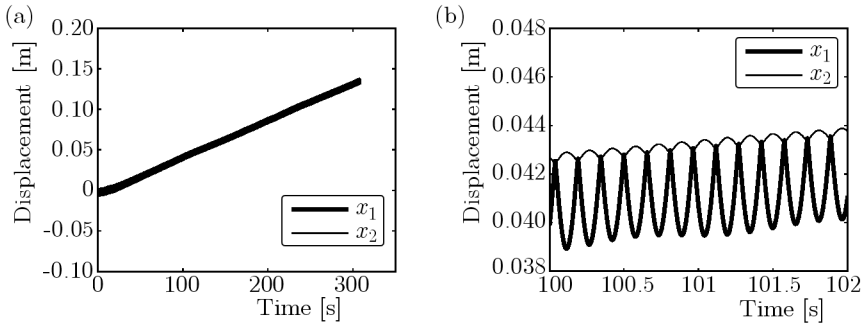

Fig. 7. Displacements of blocks 1 and 2 of the system with ideal excitation with the frequency of 6.5 Hz (a) and a detailed view showing impacts (b)

The displacements x_1 and x_2 of the system with the non-ideal excitation source are shown in Figs. 8, 9 and 10, with the frequency of 3.5 Hz, 5.5 Hz and 6.5 Hz, respectively. The displacement rates are considerably higher than for the system with ideal excitation, and this happens for all analysed frequencies. The displacement rate also tends to increase with higher excitation frequencies. However, at 6.5 Hz, the displacement increases rapidly until around 170 s, and after that it starts decreasing, although the number of impacts does not change considerably compared to the situation with 5.5 Hz, which has a higher displacement rate.

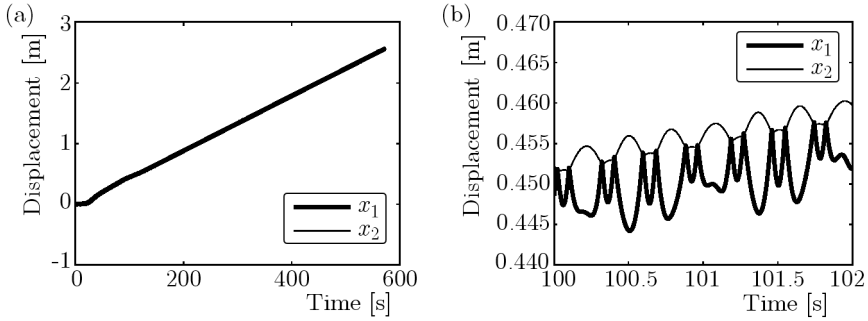

Fig. 8. Displacements of blocks 1 and 2 of the system with non-ideal excitation with the frequency of 3.5 Hz (a) and a detailed view showing impacts (b)

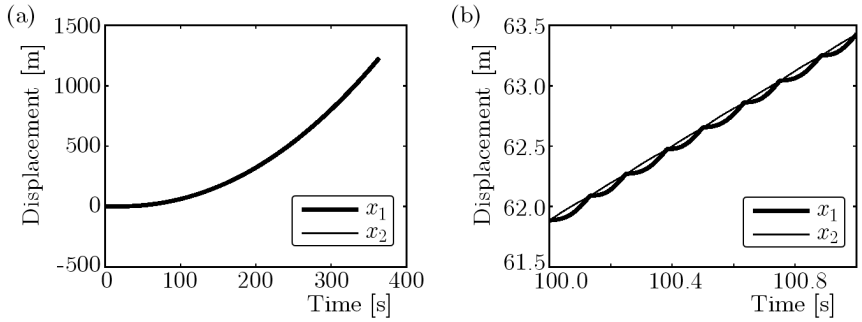

Fig. 9. Displacements of blocks 1 and 2 of the system with non-ideal excitation with the frequency of 5.5 Hz (a) and a detailed view showing impacts (b)

These results show that the models present very different results according to the type of the excitation source, ideal or non-ideal, regarding the number of impacts and the rate of displacement.

Figures 11, 12 and 13 show the phase portraits related to the frequencies of 3.5 Hz, 5.5 Hz and 6.5 Hz. The results show the large difference in displacement and velocities between the models with different excitation sources. Notice that the scales of the figures vary greatly. The displacements and velocities are much larger for the non-ideal excitation source model. For

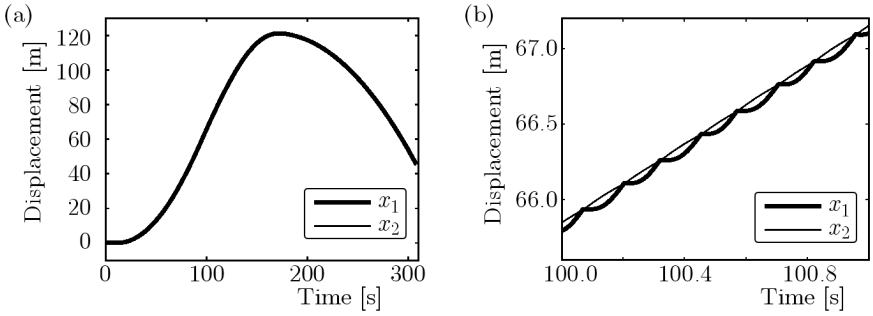

Fig. 10. Displacements of blocks 1 and 2 of the system with non-ideal excitation with the frequency of 6.5 Hz (a) and a detailed view showing impacts (b)

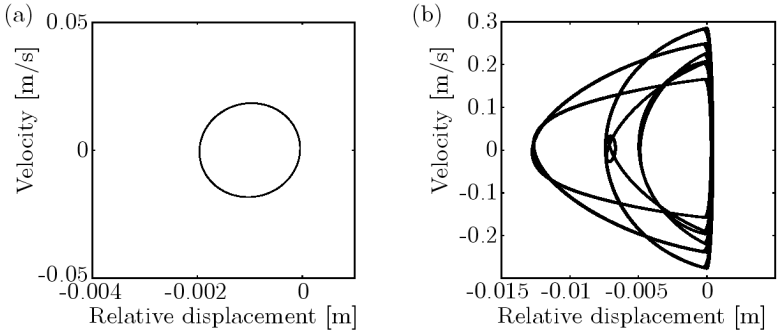

Fig. 11. Phase portraits of the systems with ideal excitation (a) and with non-ideal excitation (b) with the frequency of 3.5 Hz

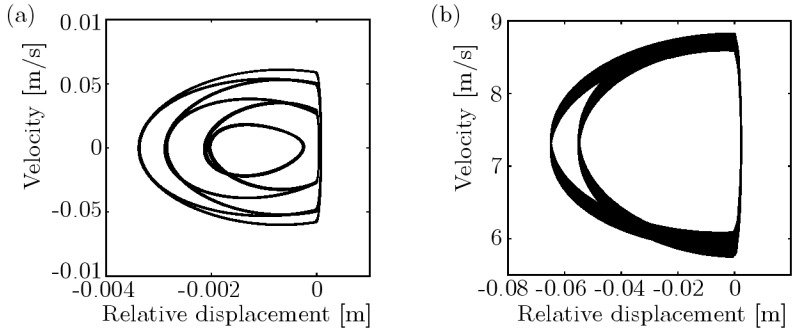

Fig. 12. Phase portraits of the systems with ideal excitation (a) and with non-ideal excitation (b) with the frequency of 5.5 Hz

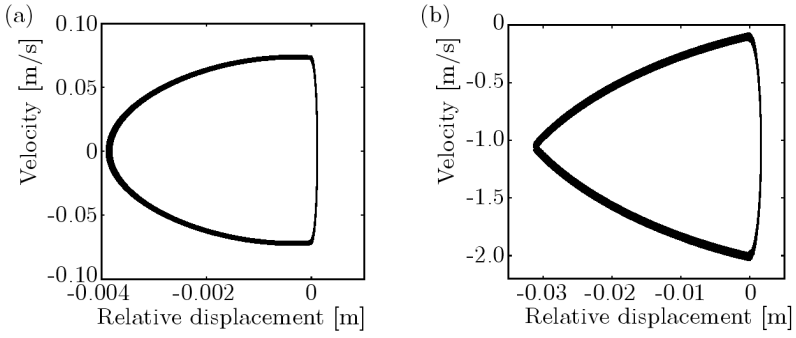

Fig. 13. Phase portraits of the systems with ideal excitation (a) and with non-ideal excitation (b) with the frequency of 6.5 Hz

both types of excitation, the phase planes tend to become more regular with higher excitation frequencies, with one impact at every cycle (period-1 limit-cycle) at 6.5 Hz.

Figures 14a, 15a and 16a show the angular velocity of the motor. Figures 15a and 16a show the influence of the system in the dynamics of the motor, called the Sommerfeld effect. In Fig. 15a, the angular velocity constant of the motor is 5.5 Hz, and the angular velocity of the motor is captured by the resonance frequency of 4.1 Hz, from which the motor cannot escape. In Fig. 16a, the angular velocity constant is 6.5 Hz, and the motor is initially captured by resonance at 4.1 Hz, but manages to overcome it and reaches the value of the angular velocity constant.

Figures 14b, 15b and 16b show the displacement with respect to the motor angular frequency. In Fig. 15b, it is possible to notice that the motor was captured by resonance (4.1 Hz) and cannot exceed this frequency, characterizing the Sommerfeld effect. In Fig. 16b, it is possible to notice that the angular frequency of the motor is captured again by resonance at 4.1 Hz, and after approximately 100 seconds, the motor reaches a sufficient condition to overcome this frequency and jumps to a frequency of approximately 6.2 Hz.

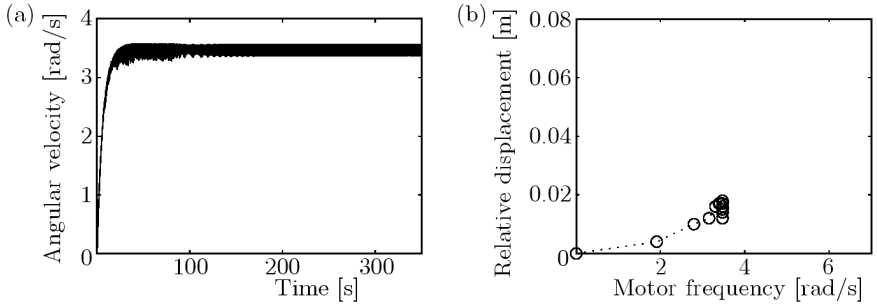

Fig. 14. Angular velocity (a) and displacement versus motor frequency of the system with non-ideal excitation with the frequency 3.5 Hz (b)

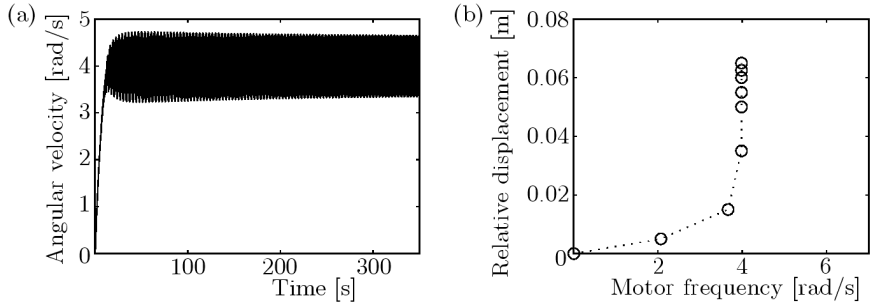

Fig. 15. Angular velocity (a) and displacement versus motor frequency of the system with non-ideal excitation with the frequency 5.5 Hz (b)

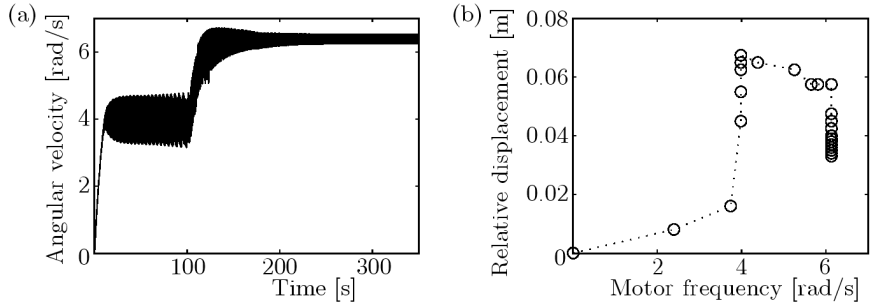

Fig. 16. Angular velocity (a) and displacement versus motor frequency of the system with non-ideal excitation with the frequency 6.5 Hz (b)

4. Conclusions

This work analyzed the dynamics of a vibro-impact system. The mechanism was modeled in two different ways with respect to the excitation source, an ideal source by means of a harmonic force, and a non-ideal source by means of a DC motor with limited power supply and an unbalanced rotor.

Although the models have similarities, the comparison between them has to be done carefully because the differences between the ideal and non-ideal excitation sources. A relationship between the forces provided by each source was defined which helped the comparison to be more realistic.

Graphs were presented for the displacement, frequency parameter, amplitude of displacement in relation to the motor rotation frequency.

The system with the non-ideal excitation source presents values of displacement and velocity much larger in relation to the model with the ideal excitation source.

Regarding the non-ideal model, three different situations were presented: in the first situation, the motor has reached a steady state angular frequency similar to the angular velocity constant of the motor, in the second and third situations, the motor exhibits the Sommerfeld effect. The analysis of the dynamics of these models showed the importance of using the non-ideal excitation source to obtain more realistic and consistent results.

Acknowledgements

The authors thank the Brazilian funding agencies FAPESP, CNPq and CAPES.

References

1. Aguiar R.R., 2010, *Experimental Investigation and Numerical Analysis of the Vibro-Impact Phenomenon*, PhD Thesis, PUC-Rio, Rio de Janeiro, Brazil
2. Balthazar J.M., Brasil R.M.L.R.F., 2004, On saturation control of a non-ideal vibrating portal frame founded type shear-building, *Journal of Vibration and Control*, **10**, 1739-1748
3. Balthazar J.M., Felix J.L.P., Brasil R.M.L.R.F., 2005, Some comments on the numerical simulation of self-synchronization of four non-ideal exciters, *Applied Mathematics and Computatuion*, **164**, 615-625
4. Balthazar J.M., Mook D.T., Weber H.I., Brasil R.M.L.R.F., Fenili A., Beltano D., Felix J.L.P., 2003, An overview on non-ideal vibrations, *Meccanica*, **38**, 613-621
5. Cvetićanin L., 2010, Dynamics of the non-ideal mechanical systems: A review, *Journal of the Serbian Society for Computational Mechanics*, **4**, 75-86
6. Dimentberg M.F., McGovern L., Norton R.L., Chapdelaine J., Harrison R., 1997, Dynamics of an unbalanced shaft interacting with a limited power supply, *Nonlinear Dynamics*, **13**, 171-187
7. Ho J.H., Nguyen V.D., Woo K.C., 2010, Nonlinear dynamics of a new electro-vibro-impact system, *Nonlinear Dynamics*, **63**, 35-49, DOI: 10.1007/s11071-010-9783-6
8. Ing J., Pavlovskaia E., Wiercigroch M., Banerjee S., 2010, Bifurcation analysis of an impact oscillator with a one-sided elastic constraint near grazing, *Physica D*, **239**, 312-321, DOI: 10.1016/j.physd.2009.11.009
9. Kononenko V.O., 1969, *Vibrating Systems with a Limited Power Supply*, Iliffe Books Ltd, London
10. Lin R.M., Ewins D.J., 1993, Chaotic vibration of mechanical systems with backlash, *Mechanical Systems and Signal Processing*, **7**, 257-272
11. Nayfeh A.H., Mook D.T., 1979, *Nonlinear Oscillations*, John Whiley & Sons, New York

12. Pavlovskaia E., Wiercigroch M., Grebogi C., 2001, Modelling of an impact system with a drift, *Physical Review E*, **64**, DOI 10.1103/PhysRevE.64.056224

13. Pontes Jr B.R., Oliveira V.A., Balthazar J.M., 2000, On friction-driven vibrations in a mass block-belt-motor with limited power supply, *Journal of Sound and Vibration*, **234**, 713-723

14. Souza S.L.T., Caldas I.L., Viana R.L.J., Balthazar J.M., 2008, Control and chaos for vibro-impact and non-ideal oscillators, *Journal of Theoretical and Applied Mechanics*, **46**, 641-664

15. Souza S.L.T., Caldas I.L., Viana R.L., Balthazar J.M., Brasil R.M.L.R.F., 2005, Impact dampers for controlling chaos in systems with limited power supply, *Journal of Sound and Vibration*, **279**, 955-965

16. Souza S.L.T., Caldas I.L., Viana R.L., Balthazar J.M., Brasil R.M.L.R.F., 2005, Basins of attraction changes by amplitude constraining of oscillators with limited power supply, *Chaos, Solitons and Fractals*, **26**, 1211-1220

17. Tsuchida M., Guilherme K.L., Balthazar J.M., 2005, On chaotic vibrations of a non-ideal system with two degree of freedom: 1:2 resonance and Sommerfeld effect, *Journal of Sound and Vibration*, **282**, 1201-1207

18. Warminski J., Balthazar J.M., Brasil R.M.L.R.F., 2001, Vibrations of a non-ideal parametrically and self-excited model, *Journal of Sound and Vibration*, **245**, 363-374

19. Wiercigroch M., Wojewoda J., Kivtsov A.M., 2005, Dynamics of ultrasonic percussive drilling of hard rocks *Journal of Sound and Vibration*, **280**, 736-757

20. Zukovic M., Cvetićanin L., 2007, Chaotic responses in a stable Duffing system of non-ideal type, *Journal of Vibration and Control*, **13**, 751-767

21. Zukovic M., Cvetićanin L., 2009, Chaos in non-ideal mechanical system with clearance, *Journal of Vibration and Control*, **15**, 1229-1246

Manuscript received October 31, 2012; accepted for print February 4, 2013